A&A 436, 325–331 (2005)
DOI: 10.1051/0004-6361:20042214


Astronomy & Astrophysics

# Inference of the magnetic field in spicules from spectropolarimetry of He I $D_3$ ⋆

A. López Ariste[1] and R. Casini[2]

[1] THEMIS. C/ Vía Láctea s/n, 38200 La Laguna, Tenerife, Spain
e-mail: arturo@themis.iac.es
[2] High Altitude Observatory, National Center for Atmospheric Research⋆⋆, PO Box 3000, Boulder, CO 80307-3000, USA

Received 20 October 2004 / Accepted 28 January 2005

**Abstract.** We present observations of spicules in the He I $D_3$ line with full-Stokes spectropolarimetry, which were done with the Advanced Stokes Polarimeter at the Dunn Solar Telescope of the Sacramento Peak Observatory. The line profiles appear to be significantly broadened by non-thermal processes, which we interpret using the hypothesis of a distribution of velocities inside the spicule. The possibility of inferring the magnetic field in those conditions is tested on synthetic data, and the results are generalized to the interpretation of the observed data. We conclude that the magnetic field is aligned with the visible structure of the spicule, with strengths above 30 G in some cases (for heights between 3000 and 5000 km above the photosphere).

**Key words.** Sun: chromosphere – Sun: magnetic fields

## 1. Introduction

Any survey of the literature on spicules would reveal a striking dichotomy between theory and observations. While theory seems to have developed at the same pace as MHD numerical techniques, the observations are basically limited (with some exceptions, see Trujillo Bueno et al. 2005 and Socas-Navarro & Elmore 2005 for recent spectropolarimetric observations of other spectral lines) to results obtained in the 1950's and 1960's. In fact, the review by Beckers (1968) already contains most of the empirical data that Sterling (2000) refers to 30 years later.

Spicules are extremely interesting features for several reasons. From the point of view of MHD theory, they almost certainly can be considered quasi-1D systems (Sterling 2000; De Pontieu et al. 2004), for which numerical solutions can easily be derived and then tested against observations. Spicules are also a visibly organized atmospheric structure in a region where the Sun's global field has probably rid itself of most of the local magnetic disturbances originating in the photosphere. In fact, spicules are generally organized in patterns that seem to reproduce the global distribution of magnetic field observed in the photospheric network. Whatever the mechanism driving the plasma ejection in the spicules, however, it is evident that they must be one of the main (if not the most important) contributors to the refueling of gas in the corona. Athay (2000) among others attributes to them a predominant role in the dynamics of the whole solar atmosphere, pointing also to the fact that the amount of matter ejected by spicules is so large that it ought to be compensated for by some kind of coronal rain, perhaps filling in the process other magnetic structures, like prominences. Finally, spicules are also interesting because they present a true observational challenge. The sub-arcsec size pushes the instrument capabilities to their limit, as one struggles to improve image quality while adversely affected by the high level of scattered light from the solar disk. This is particularly true if one is interested in acquiring spectropolarimetric data of these objects.

In this paper, we present spectropolarimetric observations of spicules done with the Advanced Stokes Polarimeter (ASP, Elmore et al. 1992) at the Dunn Solar Telescope (DST) of the Sacramento Peak Observatory (New Mexico). Spectropolarimetry requirements forced us to abandon any hope for image quality, so we lack, for instance, adequate control over distance to the limb. The limited spatial resolution also makes it difficult to disentangle the contributions by different spicules to the observed spectra. Despite these drawbacks, the observed spicules do show a strong signal in the He I $D_3$ line, both in intensity and in linear polarization. Circular polarization, even when present, is always close to the noise level. The height from the limb at which we placed the spectrograph slit had to be chosen in such a way that the solar disk would never fall onto the slit because of seeing-induced image motions. For this reason, we could not observe any lower than about 5 arcsec above the limb. As limb trackers become increasingly available to stabilize the solar image along the radial direction, we

⋆ Appendix A is only available in electronic form at http://www.edpsciences.org

⋆⋆ The National Center for Atmospheric Research is sponsored by the National Science Foundation.

should, in the near future, be able to observe spicules closer to the solar limb. Observing with an unocculted telescope that was not designed for high control of scattered light (as opposed to coronagraphs) means that we never see the upper parts of spicules.

The most obvious feature of the observed spectra in spicules, as described in Sect. 2, is the very large width of the line profiles. Any attempt to infer the magnetic field in spicules must necessarily be based on some assumption regarding the origin of such a linewidth. In this paper, we adopt the hypothesis that the only non-thermal broadening mechanism is the macroscopic distribution of velocities within the spicule. The possibility of applying our inversion procedure using this hypothesis is tested in Sects. 3 and 4. First, a database of synthetic Stokes profiles for He I $D_3$, created by a numerical code for polarized resonance scattering in the presence of magnetic fields (López Ariste & Casini 2002), is convoluted with a Gaussian with width comparable to that of the observed profiles. Next we apply our inversion code to this broadened dataset to verify that some information on the magnetic field can still be recovered. Finally, in Sect. 5 we apply our inversion procedure to the real data.

## 2. Data description

The data consist of a single time series of 33 exposures taken with the ASP at the SPO/DST. The time series extends for 4 min from 13:54 UT through 13:58 UT on May 28th, 2002. ASP modulated at 10 Hz with 64 accumulations adding up to about 6 s per exposure, all Stokes parameters considered. The slit (approximately 1 arcsec wide) was placed approximately tangent to the west solar limb at a Heliographic Position Angle of 275.9°. The distance of the slit from the H$\alpha$ limb, as seen in the slit-jaw image, is roughly 5″ or 3500 km. With the telescope pointing off the limb, we could not use any tracker that could stabilize image motion; therefore during the time series the slit sampled a region extending about 3″ in the radial direction.

Figure 6 shows one of the slit-jaw images in H$\alpha$ with the slit across the spicules and the hairlines. On the visible part of the chromosphere a bright patch may indicate a plage region with possibly enhanced photospheric magnetic fields. The spatial resolution does not allow us to tell the individual spicules apart, and we are also unable to differentiate the spicules in the plane of the sky from those in the background or in the foreground. However, we can affirm that most of them are inclined at about 40° from the radial direction, in a fashion that is well described by *wheat field pattern* (Lippincot 1957; cf. Beckers 1968). The brightest feature visible in the image was more likely a jet, since it was seen ejecting during the time series, still following the general direction at 40° from the local vertical.

The ASP was used in the configuration described by Casini et al. (2003), adopting a camera lens with a shorter focal length than the nominal one (Elmore et al. 1992). This setup allowed us to observe the Na I $D_1$ and $D_2$ lines simultaneously, along with the He I $D_3$ line. In this paper we will describe only the $D_3$ data. The position of the slit at approximately 5 arcsecs above the limb was set in response to a concern with image motion and in the hope of avoiding an excess of scattered light from the disk into the spectrograph, which greatly compromises the quality of the Stokes profiles during off-limb observations.

The observed profiles of He I $D_3$ can be characterized in the first place by their significant broadening, much larger than the typical thermal broadening, which we can tentatively attribute to macroscopic velocity distributions within the spatial resolution element. The broadening also appears to be slightly asymmetric, being larger in the red wing of the line. This is likely due to the intrinsic asymmetry of the $D_3$ multiplet, which has a larger blue component and a smaller red component (in the ratio 8:1, at the limit of optically thin plasmas). When this asymmetry is combined with the macroscopic velocity distribution of the spicules, the resulting profile will show the kind of asymmetric broadening that we see in our data. We will further discuss this broadening in the following sections.

The polarization signal is evident in Stokes $Q$ and $U$[1], whereas circular polarization (Stokes $V$) is present but not very significant. In the following sections we will discuss the possibility of extracting all possible information on the magnetic fields of spicules from the analysis of these polarization signals.

## 3. Velocity distributions

The anomalous broadenings of line profiles in spicules have been described before (Krat & Krat 1971), and often attributed to velocity distributions within the resolution element. Quite often the presence of such velocity distributions is simply determined by poor spatial resolution that mixes different physical structures in the same line profile.

Before attempting an interpretation of the observed polarization signals we must first provide a mathematical description of this broadening. We first noticed that all the observed profiles in the collected data are similarly broadened. In order to determine this we used a characteristic, thermally-broadened profile with a Doppler width equivalent to a temperature of 7500 K (as in the profile database used in López Ariste & Casini (2002) for the inversion of prominence data). This characteristic profile, $I_0(\lambda)$, was broadened according to the following algorithm,

$$I(\lambda) = \sum_{v<0} \mathrm{e}^{-(v/\Delta^-)^2} I_0(\lambda, v<0) + \sum_{v>0} \mathrm{e}^{-(v/\Delta^+)^2} I_0(\lambda, v>0). \quad (1)$$

$I_0(\lambda, v)$ indicates the characteristic profile displaced by the Doppler shift corresponding to velocity $v$. The displaced contributions are weighted by a Gaussian function with two distinct widths $\Delta^+$ and $\Delta^-$. We found in fact that a single Gaussian distribution was not sufficient to explain the observed asymmetries of the broadened profiles, so we had to adopt two different Gaussians for the red- and blue-shifted contributions. We believe this occurs because the characteristic profile, $I_0(\lambda)$ respects the theoretical ratio 8:1 between the amplitudes of the

[1] We use the customary definition of positive $Q$ indicating linear polarization tangent to the solar limb.

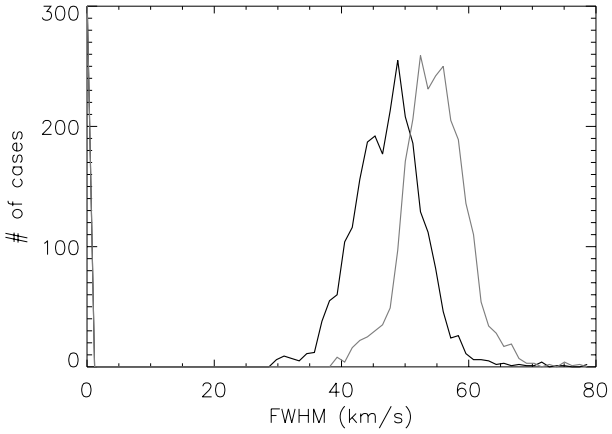


**Fig. 1.** Histograms of the *FWHM* of the two Gaussians weighting the blue- (thick line) and red-shifted (thin line) contributions as inferred from inversion of the observed He $D_3$ intensity profiles.

blue and red components of the line, whereas in the real data radiative transfer modifies this ratio towards smaller values, so the asymmetry is correspondingly affected.

We did not include radiative transfer effects here, so the only account of those effects comes through the use of a convolution with the two Gaussian velocity distributions, according to Eq. (1). A database of broadened synthetic profiles was then built by computing the profiles for different Gaussian widths $\Delta^+$ and $\Delta^-$. These two parameters were the only free parameters in the problem of finding an empirical fit to the observed Stokes *I* profiles. We solved that inversion problem by a simple code based on Principal Component Analysis (PCA) (Rees et al. 2000). The observed intensity profiles were reproduced by the broadened profiles in a very satisfactory way. In Fig. 1 we present a histogram of the results for the two parameters $\Delta^+$ and $\Delta^-$ that were allowed to vary in the inversion and see that both histograms peak very nicely at around a *FWHM* of the Gaussian of roughly 50 km s$^{-1}$.

## 4. Inversion tests with broadened databases

For the inversion of our observations we assume that line broadening is completely determined by the velocity distribution within the resolution element. We also make the further assumption that the polarization signal is not affected by the velocity distribution, that is, the Stokes profiles are broadened in the same way as the intensity profile. This is probably not completely realistic, as one could imagine that plasma that is frozen onto the field lines would show different velocities as it traces different magnetic geometries. Nevertheless we are going to proceed on the basis of that hypothesis and rely on the initial idea that the magnetic topology of spicules must be relatively simple.

The equations of the polarized emission of the He I $D_3$ line, following the single-scattering approximation used for our inversion, are given, e.g., by López Ariste & Casini (2002), where we also discuss the limits of neglecting radiative transfer for magnetic inversion. For this problem, we created a database of Stokes profiles of He I $D_3$ that covers all possible directions of the magnetic field vector and a range of field strengths up to 100 G. The number of free parameters entering the database creation is 6:3 for the vector field, 2 for the scattering geometry, and 1 for the velocity parameter introduced in the previous section. As discussed by López Ariste & Casini (2002), adopting a regular grid over the parameter space to build a database of Stokes profiles is not efficient. First of all, the resulting database would be unmanageably large. At the same time, many models would be redundant because of intrinsic ambiguities of the Hanle and Zeeman effect and because of the reduced sensitivity of the Stokes profiles in certain ranges of the model parameters. The solution proposed in that paper is to create the database through a Montecarlo iterative procedure, in which models with randomly selected parameters are first proposed and the corresponding synthetic Stokes profiles are then compared with those already accumulated in the database. If the last computed set of Stokes profiles is too similar to one already existing in the database, then it is rejected. Otherwise it is added to the database. The similarity criterium is based on PCA considerations (López Ariste & Casini 2002). A database thus built does not contain redundant models and, at the same time, keeps typically a manageable size.

For the particular problem of this paper, the selected database from the inversion of prominences was broadened using Eq. (1) with $\Delta^+ = \Delta^- \equiv 50\,\mathrm{km\,s^{-1}}$; and we attempted to invert this modified database with the original, unbroadened database. This is the best case possible, since the actual models for each individual case are present in the original database. Figures 2 and 3 show the results of this inversion for the azimuth and inclination in the line-of-sight (LOS) reference frame[2], and for the field strength.

From the inversion histograms we see that the azimuth in the LOS reference frame is still fairly well recovered, in spite of the increased inversion errors that are in most cases below 10° from the true solution (the 180° ambiguity is easily distinguished in the histogram as a secondary peak). Information on the inclination of the magnetic field, instead, is almost completely lost in the broadening process, with error bars around 40°. The field-strength information also seems to be lost at first glance. However, error increases with the field strength (right plot in Fig. 3), which allows us to conclude that the inversion should still be able to tell the presence of weak fields in spicules, as they would be inverted with comparably weak (or at most average) fields. As an example, for a true field-strength of 20 G, the inversion code will not, on average, retrieve solutions above 40 G. On the other hand, the inversion solution corresponding to a true strong field could fall anywhere within the magnetic field range accessible to the inversion code.

From the previous tests we can expect the inversion code to provide information on the azimuth of the field in the LOS reference frame. We can also expect to tell the following two cases apart: those in which only weak fields (under 20 G) are present in spicules and those in which strong fields can also be found.

[2] For a graphical definition of the local and LOS reference frames, as well as of the angles in each one of those frames, please refer to Fig. 1 of Casini (2002) or López Ariste & Casini (2002).

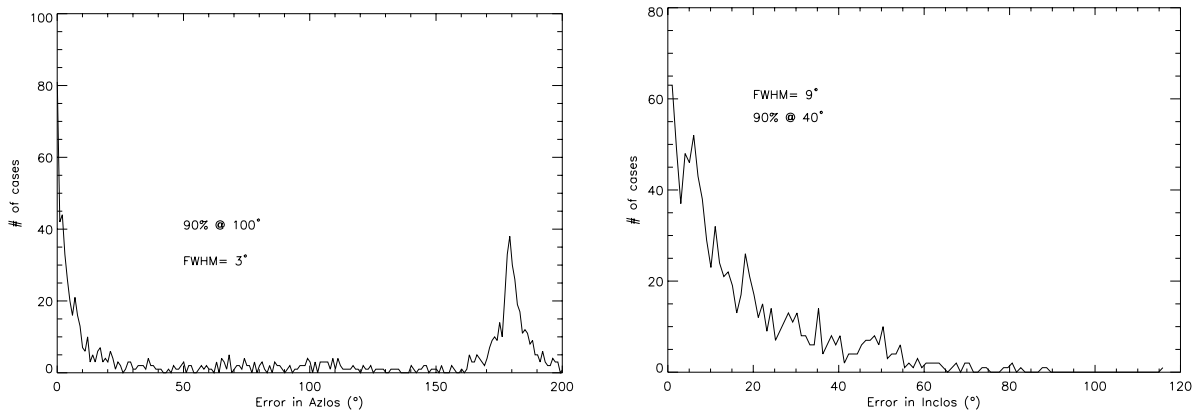


**Fig. 2.** Histograms of the errors for the inversion of a broadened database of profiles (the "observations") with the original, unbroadened database. On the left, azimuth of the magnetic field in the LOS reference frame (defined by the line-of-sight and the meridional plane through the scattering point), and on the right, the magnetic inclination in the same reference. Estimates of the *FWHM* of the error distribution and of the 90% level are given in the figure.

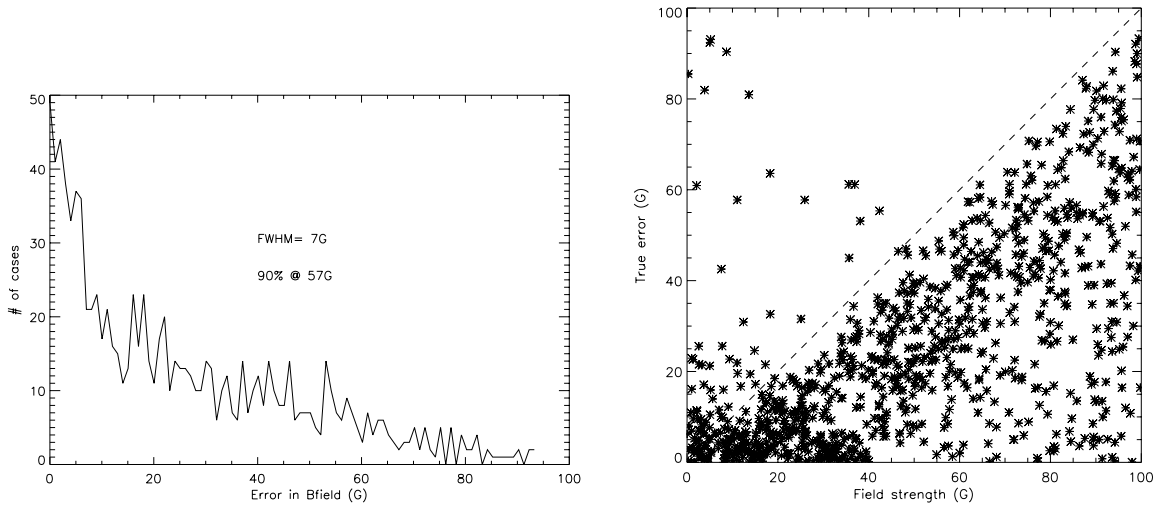


**Fig. 3.** On the left panel, histogram of the error in field strength for inversion of broadened synthetic profiles with the original unbroadened database. On the right, scatter plot of the errors in the inverted field strength as a function of the true field strength, showing that error increases with field strength.

If strong fields are retrieved, however, we cannot say much about the possible presence of weak fields.

Before applying the inversion code to real data, we want to comment on the results of another test performed on the broadened, synthetic profiles. A common feature of our real data is that the Stokes-$V$ signals have small amplitudes compared to observation noise, and they also appear very distorted. As a consequence, one can expect that these signals will not contribute significantly to the inversion process. It is well known (López Ariste & Casini 2002; Brown et al. 2003) that neglecting Stokes $V$ in the polarization analysis of He I $D_3$ increases the inversion errors for both field strength and geometry. However, we also find that this introduces new ambiguities into the inversion results. Specifically, we find 90° ambiguity in the inverted values of the field azimuth in the LOS reference frame (Casini et al. 2005).

In Fig. 4 we see that this ambiguity is not as prominent in the inversion error histograms as the one at 180°, but it still can determine perpendicular solutions for the direction of the magnetic field in the plane of the sky, whenever Stokes $V$ is not significant.

## 5. Application to the observed data

Following the hypotheses stated in the previous section, we applied our inversion code with the unbroadened database to the real data. To be consistent with the conclusions from our tests on synthetic profiles, we only report the results on field strength and azimuth in the plane of the sky.

For the azimuth of the field in the LOS frame of reference, we limited the possible range between −90° and 90°, thus avoiding the problem of 180° ambiguity. Because of this ambiguity, the azimuth values will only indicate direction of the projection of the field on the plane of the sky, but not its polarity.

We also observe the presence of the additional 90° ambiguity in our results, which we attribute to the small significance of Stokes $V$ in our data (see previous section). Therefore, the

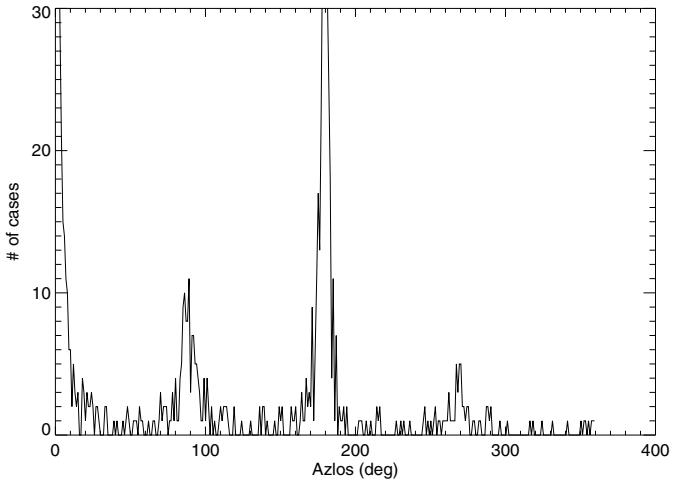


**Fig. 4.** Histogram of errors in the inversion of the magnetic-field azimuth in the LOS reference frame, excluding Stokes $V$ from the inversion. The database used for this figure is composed of the artificially broadened profiles described previously.

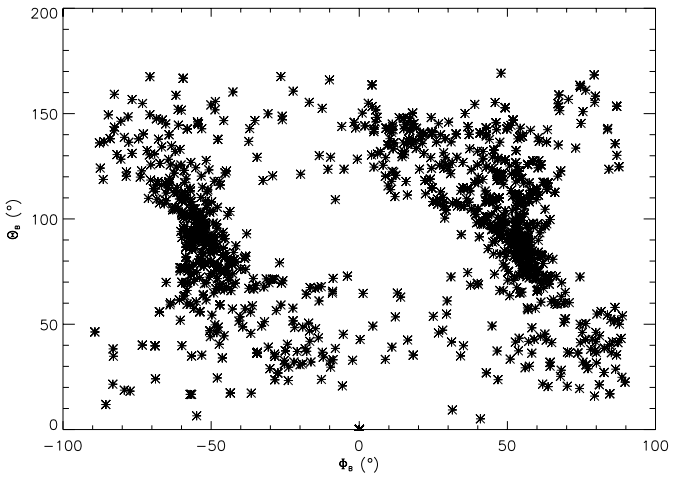


**Fig. 5.** Plot of inferred inclination $\Theta_B$ in the local frame vs. azimuth $\Phi_B$ in the LOS frame.

field is either aligned with the projected axis of the spicule on the plane of the sky, or perpendicular to it.

Figure 5 shows the distribution of inclination $\Theta_B$ and azimuth $\Phi_B$ of the magnetic field in the LOS reference frame for the inverted data. We opted for the LOS reference frame, because in it the 90° ambiguity is more easily grasped (see the appendix), and in fact we notice the presence of two groups of solutions roughly centered at $(\Phi_B, \Theta_B) = (\pm 50°, 90°)$ in Fig. 5. In the appendix, we show the regions of the $(\Phi_B, \Theta_B)$ plane that can be subject to the 90° ambiguity. We then see that the dense cluster around $(\Phi_B, \Theta_B) = (-50°, 90°)$ corresponds to solutions that are mostly unambiguous. This is not the case for the cluster around $(\Phi_B, \Theta_B) = (50°, 90°)$, which instead is mapped via the 90° ambiguity onto the lower part of the leftmost group of solutions. For the 90° ambiguous solutions, we arbitrarily selected the value of $\Phi_B$ that approximately aligns the projection of the magnetic field on the plane of the sky with the observed spicule. However, we must keep in mind that an ambiguous solution giving a field approximately perpendicular to the axis of the spicule cannot be excluded a priori on the basis of the observations.

Figure 6 shows Exposure # 19 as a sample of our data. We plotted the inverted solution for the plane-of-the-sky projection of the magnetic field over a slit-jaw image in H$\alpha$. Each solution vector field corresponds to the spicular feature behind the slit at the same horizontal position. The brightness of each segment is proportional to the intensity brightness of the feature in the core of the He I $D_3$ line, thus makin identification of the various structures easier. The length of the segments is proportional to the inverted field strength. Inclination of the segments with respect to the vertical (perpendicular to the slit) is the azimuth $\Phi_B \pm 180°$. Because the error bars in the inverted values of $\Phi_B$ are well below 10 degrees, we can conclude that the presence of magnetic fields roughly aligned with the observed structures (or perpendicular to them!) is the most reliable conclusion drawn from our data.

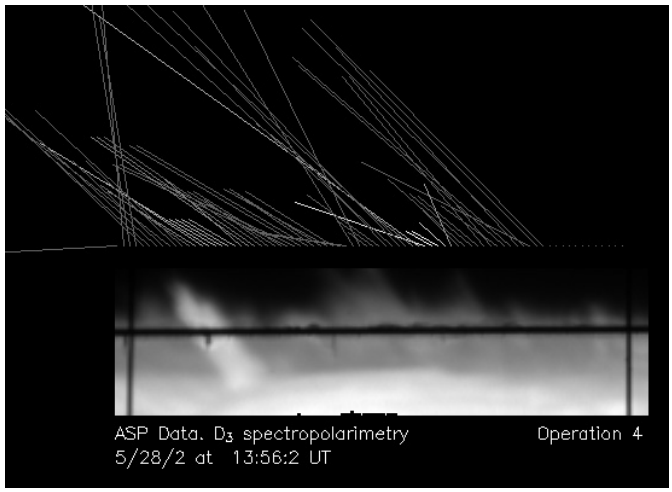


**Fig. 6.** Exposure # 19 of the time series. In the background, the slit-jaw image in H$\alpha$ showing the position of the slit (horizontal) over the spicules. The distance between the hairlines is 1 arcmin exactly with spatial resolution of 0.29 arcsec/pixel. The slit was opened to slightly over 1 arcsec. Superimposed on the same column (with a vertical offset), we also plot the inverted solution for the magnetic field vector for each point on the slit. The direction of the lines is given by the azimuth in the LOS reference frame, and their length by the field strength. The level of gray of each line is scaled according to the intensity of the observed feature in the slit-jaw image.

As anticipated, the error bars on the magnetic strength are much larger, as they grow proportionally to the strength, so the inferred values cannot be considered very significant. A better picture of the distribution of magnetic strengths in our inverted data is shown in Fig. 7. Retrieval of strong fields in our inversion indicates that such fields must actually be present at a statistically significant level, because weaker fields, which are affected by proportionally smaller errors, cannot produce the polarization signature that the inversion algorithm attributes to the stronger fields. Statistically, strong fields above 30 G (and probably 40 G too) must therefore be present in spicules, although they may happen to occur only in a minority of cases.

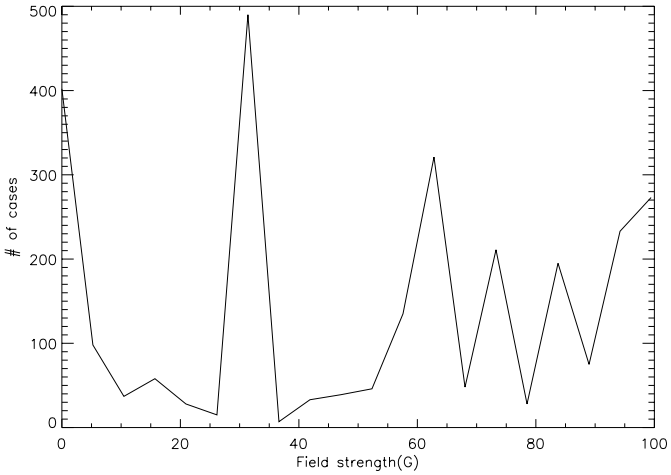


**Fig. 7.** Distribution of field strengths from inversion of the Stokes parameters plotted in 5 G bins.

In particular, because of the large error bars, we cannot tell if, for any specific point in our data, a large value of the inverted strength actually corresponds to the presence of such strong field at that point. In contrast, small values of inverted strengths are more reliable.

To compare the range of magnetic field strengths in spicules determined from our observations with typical field strengths adopted in MHD simulations of these structures we considered two of the most recent papers, among the few references in the literature on spicule modeling that report on the field strength values adopted for the numerical model. In the paper by De Pontieu et al. (2004), the magnetic field decreases from 1600 G in the photosphere to 120 G in the corona, above the spicules. Despite the title of that paper, it is clear that the authors refer mostly to fibrils that arise from active regions, rather than to quiet sun spicules. It is not clear to us if the model would lead to formation of spicules even for the weaker magnetic strengths inferred from our observations.

In James et al. (2003) on the numerical simulation of Alfvén waves generating and supporting spicules, the authors compute maximum spicule heights for different magnetic fields in the corona, and for several different wave periods from 2 to 10 s. Our inferred field strengths hardly allow coronal field strengths that reach a 20 G value, which seems right at the limit of what those authors would need to reproduce spicule heights. On the other hand, the spicule heights that they compute for 10 G coronal fields, which seems a more appropriate value for the range of field strengths in spicules that we inferred, appear to be too low compared to observed spicular heights.

Finally, all these works mostly assume magnetic fields aligned with the spicular structures. However, from our observations of He I $D_3$ in spicules and because of the 90° ambiguity, we cannot exclude the possibility of a magnetic field transversal to the spicule axis. Such transversal fields could be of interest to explain those velocity fields we needed to introduce in order to reproduce the anomalous broadening of the observed profiles.

## 6. Conclusion

Spectropolarimetric observations of spicules in the He I $D_3$ line taken with the Advanced Stokes Polarimeter allowed us to investigate the possibility of measuring the magnetic field in those structures. The anomalous broadening of the line profiles, which we find in our data and attribute to the presence of velocity distributions within the resolution element, represents the biggest challenge for interpretating those data. In order to attempt inversion of the observations, we had to make two fundamental assumptions: that radiative transfer effects are absent, and that the polarization signature in a profile is not affected by velocity distributions. It is known that the first hypothesis does not strictly apply, because previous observations in prominences of the He I $D_3$ line show evident departure from the optically thin regime, and because the line asymmetry in the spicule observations cannot be fully accounted for by the presence of the red component. We were able to reproduce the observed intensity profiles by introducing two Gaussian distributions of velocities with mean *FWHM* centered at 50 km s$^{-1}$ for the blue and red components of the line, respectively, where the red distribution must be wider to account empirically for the radiative-transfer induced asymmetries.

The validity of the second hypothesis is not tested, but is equivalent to assuming that the magnetic topology and irradiation conditions are identical in the emitting plasma independently of its velocity, which is questionable for plasma that is frozen onto the magnetic field lines. Tests run with synthetically broadened data show that, despite broadening, the inversion code is still able to infer the direction of the projection of the field on the plane of the sky with relatively good precision, apart from the 90° ambiguity that can affect particular magnetic inclinations. Tests also show that, although the field strength information is lost because of the very large line broadening, the maximum inversion errors appear to be proportional to the true field strength. Therefore, if only weak fields are present in the spicules, the inversion code will on average retrieve the correct order of magnitude of the field. If instead strong fields are also present, statistically the inversion code will invert them with both small and large inverted values of the field strength.

We analyzed the data of 35 exposures of spicules at an approximate height of 5 arcsec above the limb taken with the ASP at the DST of the Sacramento Peak Observatory. The results suggest that the magnetic field in spicules is aligned with the axis of the observable structures in intensity. A 90° ambiguity that cannot be resolved with the present data also allows for solutions presenting a magnetic field transversal to those structures. We chose the first set of solutions with an aligned magnetic field with which theoretical models may agree better, but we stress that from the point of view of spectropolarimetry the transversal solution is also valid. Finally, we could infer that fields of the order of 40 G are likely to be present in spicules, although weaker fields (10 G) are probably more common. The inferred fields seem to be on the lower boundary of the acceptable range of field strengths for most of the present spicule models.

## References

Athay, R. G. 2000, Sol. Phys., 197, 31
Beckers, J. M. 1968, Sol. Phys., 3, 367
Brown, A., López Ariste, A., & Casini, R. 2003, Sol. Phys., 215, 295
Casini, R. 2002, ApJ, 568, 1056
Casini, R., & Judge, P. 1999, ApJ, 522, 524
Casini, R., López Ariste, A., Tomczyk, S., & Lites, B. 2003, ApJ, 598, L67
Casini, R., Bevilacqua, R., & López Ariste, A. 2005, ApJ, in press
De Pontieu, B., Erdélyi, R., & James, S. P. 2004, Nature, 430, 536
Elmore, D., Lites, B., Tomczyk, S., et al. 1992, in Proc. SPIE, 1746, 22
James, S. P., Erdélyi, R., & De Pontieu, B. 2003, A&A, 406, 715
Krat, V. A., & Krat, T. V. 1971, Sol. Phys., 17, 355
López Ariste, A., & Casini, R. 2002, ApJ, 575, 529
Rees, D., López Ariste, A., Thatcher, J., & Semel, M. 2000, A&A, 355, 759
Socas-Navarro, H., & Elmore, D. 2005, ApJ, 619, L195
Sterling, A. C. 2000, Sol. Phys., 196, 79
Trujillo Bueno, J., Casini, R., Landolfi, M., & Landi Degl'Innocenti, E. 2002, ApJ, 566, L53
Trujillo Bueno, J., Merenda, L., Centeno, R., Collados, M., & Landi Degl'Innocenti, E. 2005, ApJ, 619, L191

# Online Material

Article published by EDP Sciences and available at http://www.edpsciences.org/aa or http://dx.doi.org/10.1051/0004-6361:20042214

## Appendix A: The 90-degrees ambiguity

The physics of resonance scattering polarization in the presence of a magnetic field, which accounts for phenomena like the Hanle effect, shows that some ambiguities can affect the polarization signals that are produced in a scattering process, so that different magnetic configurations may result in identical Stokes profiles, at least from the observational point of view. Some of these ambiguities are very well known, like the ubiquitous 180° ambiguity in the POS direction of the magnetic field in the Zeeman effect, or the insensitivity of resonance polarization to the strength of vertical fields in the Hanle effect regime[3]. In the Hanle effect, the 180° ambiguity is also present in the two limit cases of forward scattering and 90° scattering (see, e.g., Casini 2002). Other ambiguities are less known, simply because less common. One of these is a 90° ambiguity also affecting the plane-of-the-sky direction of the magnetic field and arising in very specific cases (see, e.g., Casini & Judge 1999). For the sake of simplicity, we show how this ambiguity comes about in the case of a two-level atom in the saturated regime of the Hanle effect using analytic expressions derived by Casini (2002). This restricted case can then be used as a basis for understanding how this ambiguity is produced in more general cases.

Equations (A1a-d) in Casini (2002) give explicit expressions of the emission in the four Stokes parameters for the case under study. The saturated regime of the Hanle effect is defined by the condition

$$\frac{g\omega_B}{A} \gg 1, \tag{A.1}$$

where $g$ is the Landé factor of the level, $\omega_B$ the Larmor frequency of the ambient field, and $A$ the Einstein coefficient for spontaneous emission from the upper level of the transition. In this condition, the emissivity of Stokes $Q$ and $U$ no longer depends on field strength, but only on geometry,

$$\varepsilon_Q \approx \frac{3}{8} w(3\cos^2\vartheta_B - 1)\sin^2\Theta_B \cos 2\Phi_B \tag{A.2}$$

$$\varepsilon_U \approx \frac{3}{8} w(3\cos^2\vartheta_B - 1)\sin^2\Theta_B \sin 2\Phi_B. \tag{A.3}$$

Here we indicate the inclination of the field in the reference frame of the local vertical as $\vartheta_B$ and the one in the line-of-sight (LOS) reference frame as $\Theta_B$. In this LOS reference frame, the azimuth is $\Phi_B$. Finally, $w$ is the anisotropy factor of the light from the photosphere illuminating the atom.

In this regime, the 180° ambiguity appears naturally in the factor 2 that multiplies the azimuth $\Phi_B$ in all the expressions. We further realize that a 90° change in $\Phi_B$ introduces only a change of sign in all expressions, which can be masked by a sign change of the factor $(3\cos^2\vartheta_B - 1)$, which may occur for a different geometry of the magnetic field. One realizes that this is not possible for all azimuths. Figure A.1 shows the domain $(\Theta_B, \Phi_B)$ where the ambiguity can occur. Two solutions that are 90° apart in $\Phi_B$ are ambiguous (in the sense of the 90° ambiguity) only if the corresponding value of the $Z$ function is the same (i.e., identical color in the contour plot).

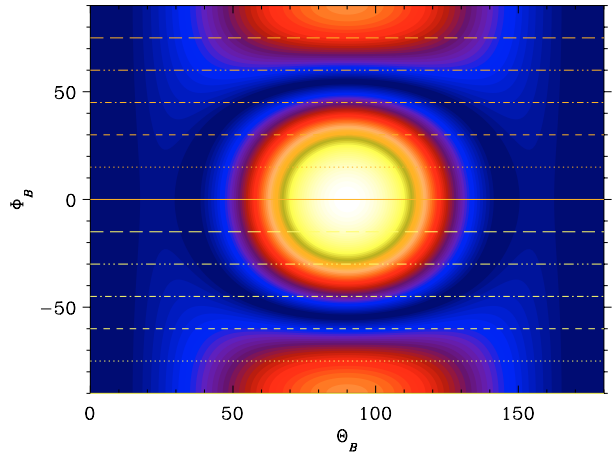


**Fig. A.1.** Contour plot of function $Z(\Theta_B, \Phi_B) = 3\sin^2\Theta_B \times (\sin^2\Theta_B \cos^2\Phi_B - 1)$ in terms of inclination $\Theta_B$ and azimuth $\Phi_B$ in the line-of-sight reference frame. Contours delimit the connected region of the plane where 90° ambiguity is possible.

This ambiguity is inevitable if there is no independent manner of determining the sign of the $(3\cos^2\vartheta_B - 1)$ factor. In principle, in the case of the saturated regime of the Hanle effect, this is achieved by means of full spectropolarimetric observations, therefore acquiring data in all four Stokes parameters $I$, $Q$, $U$, and $V$. If Stokes $V$ is not observed, the 90° ambiguity becomes inevitable. In fact, since in practice we never model the true amplitude of Stokes $I$ (i.e., with relative, rather than absolute, spectropolarimetry), the full Stokes vector of one line is not sufficient to completely avoid 90° ambiguity. In the depolarization regime of the Hanle effect, when the field strength is such that

$$\frac{g\omega_B}{A} \sim 1, \tag{A.4}$$

the dependence of Stokes $Q$ and $U$ on the magnetic strength introduces sufficient information to resolve in principle the 90° ambiguity. A more detailed investigation of the occurrence of the 90° ambiguity in the inversion of spectropolarimetric data is given in Casini et al. (2005).

After extrapolating these results to the case of the He $D_3$ line, we conclude that the presence of the two components and observation of Stokes $V$ typically mean one is able to resolve this 90° ambiguity (e.g., in quiescent prominences; see López Ariste & Casini 2002 and Casini et al. 2003). In the case of spicules, however, the broadening of the observed profiles implies that the two components of the line are indistinguishable. At the same time, Stokes $V$ profiles are driven too near to noise level in almost any configuration, thus diminishing their relevance to the problem. It is thus not surprising that we see the 90° ambiguity affecting the inversion of our data under these conditions.

[3] This is strictly true only for multi-level atoms where quantum interferences between levels with different total angular momentum are negligible (see, e.g., Trujillo Bueno et al. 2002).